cm^{-3} sec^{-1} at which $\Delta t < 10$ sec, it follows that $\sigma_h > 10^{-13}$ cm^2 for $N_h = 10^{19}$ cm^{-2} and $\lambda \simeq 10^{-6}$ cm.

This large capture cross section requires Coulomb-attractive hole traps which need to keep the holes trapped at fields larger than E_{II}. Therefore, they must be deeper than the quasi Fermi level for holes in the bulk. Shallower hole traps are already ionized by an extended Frenkel-Poole mechanism[35] for fields $E < E_{II}$ (see Ref. 35). However, these deep hole traps would certainly have to be filled by the given optical excitation at low fields in the crystal bulk, necessitating an equal density of trapped electrons (10^{19} cm^{-3}). Thermally stimulated currents and photoconductivity rise time (from initial thermal equilibrium) are at least two orders of magnitude smaller than required for these high trap densities.

Therefore, marked electron tunneling through the barrier at the cathode can be neglected.

[35] K. W. Böer, G. A. Dussel, and P. Voss, Office of Naval Research Technical Report No. 22 NONR (G) 4336 (00), 1968 (unpublished); Bull. Am. Phys. Soc. 13, 95 (1968); K. W. Böer and G. A. Dussel (unpublished).

PHYSICAL REVIEW VOLUME 179, NUMBER 3 15 MARCH 1969

Interaction between a Neutral Atomic or Molecular Beam and a Conducting Surface*

D. RASKIN AND P. KUSCH
Columbia Radiation Laboratory, Department of Physics, Columbia University, New York, New York 10027
(Received 7 October 1968)

The deflection of a beam of neutral atoms by an uncharged conducting surface has been observed. This deflection is a result of the attraction between the instantaneous electric dipole moment of an atom in the beam and the image dipole induced in the metal. The measured deflections agree in form and magnitude with those predicted from theoretical interaction potentials. Changes in the geometry of the deflecting surface give results that are in agreement with predictions. The deflection of a beam of polar molecules by metal and dielectric surfaces has also been observed. It can be explained by the interaction between the surface and the total instantaneous electric dipole moment of the molecule, including one characterized by motion at the frequency of molecular rotation, and one by motion at electronic frequencies.

INTRODUCTION

A NEUTRAL atom will be attracted to a conducting surface through the interaction between the rotating electric dipole moment of the atom and the image dipole induced in the metal. The interaction depends not only upon atomic properties and the separation between atom and surface but also upon the properties of the metal. These determine how well the image dipole follows the rapid fluctuations of the atomic electrons. An interaction energy of the form

$$V = -k/R^3 \tag{1}$$

has been proposed by Lennard-Jones,[1] Bardeen,[2] and Mavroyannis[3] for an atom near an infinite plane surface, where R is the distance between the atom and the surface and k is a constant.

Lennard-Jones assumed that the metal is a perfect conductor at all frequencies and derived the result

$$k_{L\text{-}J} = \tfrac{1}{12} e^2 \langle r^2 \rangle_{av}, \tag{2}$$

where $\langle r^2 \rangle_{av}$ is the mean-square displacement of electrons in the atom and e is the electronic charge. Both Bardeen and Mavroyannis have examined a more realistic model of the interaction in which the finite conductivity of the metal is included as well as the frequency of the photons exchanged between metal and atom. In the case of an atom in an S ground state whose spectrum is dominated by a single transition from the ground state, their results can be written in the form

$$k = k_{L\text{-}J}\eta/(1+\eta), \tag{3}$$

with the quality η given as

$$\eta_B = Ce^2/2r_s\Delta \tag{4}$$

and

$$\eta_M = \hbar\omega_p/\Delta\sqrt{2} \tag{5}$$

by Bardeen and Mavroyannis, respectively. C is a dimensionless number calculated by Bardeen to be approximately equal to 2.6 for ordinary monovalent metals; r_s is the radius of a sphere in the metal containing one conduction electron; Δ is the energy of the dominant atomic transition from the ground state; and ω_p is the plasma frequency of the metal ($\omega_p^2 = 4\pi Ne^2/m$, where N is the density of conduction electrons and m is the electronic mass).[3] If we use the approximation $N \approx 3/(4\pi r_s^3)$, then $\eta_M \approx \eta_B (a_0/r_s)^{1/2}$, where a_0 is the

* This work was supported in part by the U. S. Army Research Office, Durham, under Grant No. DA-ARO-D-31-124-G-972, and in part by the Joint Services Electronics Program under Contract No. DA-28-043 AMC-00099(E).

[1] J. E. Lennard-Jones, Trans. Faraday Soc. 28, 334 (1932).
[2] J. Bardeen, Phys. Rev. 58, 727 (1940).
[3] C. Mavroyannis, Mol. Phys. 6, 593 (1963).

Bohr radius. Since the quantity η becomes large for good conductors and low transition frequencies, (4) and (5) reduce to (2) in its region of validity, and $k_{L\text{-}J}$ is an upper limit to the interaction constant.

Margenau and Pollard[4] have calculated the energy for an atom whose dominant transition energy Δ is greater than the energies of the principal absorption bands of the metal, as in the case of light inert gases with most good conductors. Their result is also of the form (1). In the present experiment a beam of atomic Cs is deflected by a gold surface and the condition of Margenau and Pollard is not satisfied. Casimir and Polder[5] have shown that the effect of electromagnetic retardation in the Lennard-Jones approximation when the separation R is large compared with the wavelength λ of a typical atomic transition is to change the R dependence of the interaction energy to R^{-4}. In the present experiment R is of the order of $\frac{1}{10}\lambda$, so that the potential is well approximated by the form (1).

Our measurements of the interaction constant k for a Cs beam and a gold surface is consistent with the expressions given by Bardeen and by Mavroyannis. It is to be noted, however, that our measurements are not sufficiently accurate to enable us to determine η well enough to allow a critical test of the validity of the expressions (2)–(5) to be made.

The derivation of the force by Mavroyannis is analogous to a calculation by Lifshitz[6] of the force of attraction between two uncharged surfaces. The results of Lifshitz have been experimentally verified by Derjaguin *et al.*[7] in an experiment in which the force between an uncharged conducting plane and a sphere was measured directly.

Attempts have been made[8] to relate measurements of the heat of physical adsorption of an atom on a clean surface to the theoretical models of the atom-surface interaction. The relevance of the formulas [Eqs. (2)–(5)] to physical adsorption is not clear, however, since the center of an adsorbed atom is at a distance from the metal which is comparable to the lattice spacing and thus the conductor does not appear to be continuous.

The present experiment was preceded by an unsuccessful attempt at the Columbia Radiation Laboratory to measure the attraction of an atomic beam by a plane surface.[9]

The formulas given in the preceding discussion apply only to atoms or to molecules with no permanent electric dipole moment. Margenau and Pollard[4] predict that since the rotation of a polar molecule and hence of the permanent dipole of the molecule is relatively slow (rotational frequency $\approx 2\times 10^{11}$ Hz), the average interaction between a polar molecule and a metal surface can be described by the simple Lennard-Jones potential ($k=\frac{1}{12}\mu^2$, where μ is the permanent dipole moment). We have found that the interaction between CsCl molecules and a gold surface cannot be explained on this basis alone. Presumably, there is a contribution to the attraction which is due to the interaction between the surface and instantaneous dipoles such as those which give rise to the attraction between an atom and a surface.

OUTLINE OF EXPERIMENT

The most obvious experiment to detect the interaction of a neutral particle with a conducting surface is one in which the surface is a plane. An atomic beam in which all the particles move in virtually the same direction and which is uniform at all relevant distances from the plane is partially intercepted by the block on which the test plane appears, and the intensity distribution within the geometrical shadow of the block (the beam "profile") is measured. To interpret the distribution in the shadow, it is necessary to know the angle of the plane with respect to the beam velocity. This cannot be independently known or adjusted to the necessary precision. Accordingly, in the present experiment, a cylindrical surface of large radius is used as the deflecting surface. Particles approach the cylinder with all relevant impact parameters, and no parameters that need to be independently determined occur.

A beam of neutral atoms evaporated from a molecular beam oven is defined by a narrow slit S_1 (Fig. 1). Because the oven slit is wide (0.01 cm) relative to the 10-μ (0.001-cm) defining slit S_1, the beam diverges from the 10-μ slit. The beam width is approximately 0.03 cm as it passes the cylinder; thus, the surface interacts with particles with a large range of impact parameters. Particles with impact parameters a larger than about 1000 Å will be deflected through an unmeasurably small angle. The deflection increases much more rapidly than linearly as the impact parameter is decreased. Thus there is a rapidly decreasing intensity per unit width in the detector plane for increasing

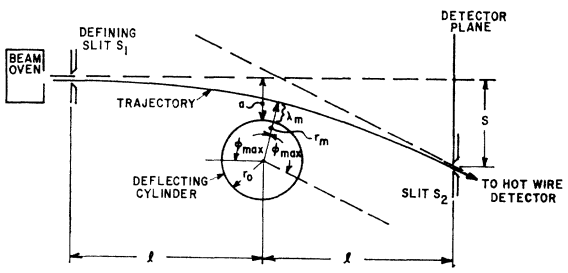

FIG. 1. Beam particle trajectory (deflection exaggerated for clarity). Top view.

[4] H. Margenau and W. G. Pollard, Phys. Rev. **60**, 128 (1941).
[5] H. B. G. Casimir and D. Polder, Phys. Rev. **73**, 360 (1948).
[6] E. M. Lifshitz, Zh. Eksperim. i Teor. Fiz. **29**, 94 (1955) [English transl.: Soviet Phys.—JETP **2**, 73 (1956)].
[7] B. V. Derjaguin, I. I. Abrikosova, and E. M. Lifshitz, Quart. Rev. (London) **10**, 295 (1956).
[8] R. A. Pierotti and G. D. Halsey, J. Phys. Chem. **63**, 680 (1959); H. Chon, R. A. Fisher, R. D. McCammon, and J. G. Aston, J. Chem. Phys. **36**, 1378 (1962).
[9] F. Cook and I. I. Rabi, Columbia Radiation Laboratory Progress Reports No. 4-12, 1960–1962 (unpublished).

deflection angles. For an impact parameter less than about 500 Å, in a typical case, a particle will strike the surface. Thus only an extremely narrow part (several hundred Å) of the total incident beam width appears in the geometrical shadow of the cylinder within a width of several tenths of a millimeter, and the intensities to be measured will be very low.

The fact that impact parameters greater than ≈ 1000 Å yield no significant deflection allows the use of the potential in Eq. (1) in which retardation effects are ignored in the analysis of the deflected beam intensities. Further, since all impact parameters are much less than the cylinder radius, the instantaneous image of the dipole is that induced in an infinite conducting plane. The minimum impact parameter is large compared with the lattice spacing of the surface so that the atom "sees" a continuous conductor.

The trajectory of a particle that approaches the cylinder of radius r_0 with an impact parameter a can be found by use of classical orbit theory. We define the constant $\beta=k/E$, where E is the kinetic energy of the particle.

The deflection s is given by (see Fig. 1 for definition of symbols)

$$s=l(2\varphi_{\max}-\pi),$$

where

$$\varphi_{\max}=\int_{r_m}^{\infty}\frac{dr}{r[F(r)]^{1/2}}, \tag{6}$$

and

$$F(r)=\frac{r^2}{(r_0+a)^2}+\frac{\beta r^2}{(r_0+a)^2(r-r_0)^3}-1,$$

where r is the distance of the particle from the cylinder axis.

The minimum distance r_m of the orbit from the cylinder axis is found from $F(r_m)=0$. We write $r_m=r_0+\lambda_m$, where λ_m is the closest distance of approach to the cylinder surface. Then

$$\lambda_m^3(a-\lambda_m)=\tfrac{1}{2}\beta r_0 \tag{7}$$

to a very high degree of approximation since $a,\lambda_m \ll r_0$. It can be shown that Eq. (7) has a real solution, λ_m only if the impact parameter a is greater than a_1, where a_1 is given by

$$a_1=\tfrac{4}{3}(\tfrac{3}{2}\beta r_0)^{1/4}.$$

Particles with impact parameters less than a_1 are captured by the surface and thus do not reach the detector. The minimum value of λ_m is given by

$$\lambda_{m\,\min}=\tfrac{3}{4}a_1.$$

It is not possible to integrate the expression for $\varphi_{\max}$ [Eq. (6)] directly in terms of elementary functions, but we have been able to derive[10] the following infinite series for s to the order of $(\delta/r_0)^0$, where $\delta=a-\lambda_m=\beta r_0/2\lambda_m^3$. The first five terms of the series are

$$s=\frac{15\pi l}{8\sqrt{(2r_0)}}\frac{\delta}{\sqrt{\lambda_m}}[1+1.192(\delta/\lambda_m)+2.285(\delta/\lambda_m)^2+5.054(\delta/\lambda_m)^3+12.02(\delta/\lambda_m)^4+\cdots], \tag{8}$$

where the coefficients of the quantities $(\delta/\lambda_m)^k$ are rational numbers. As the impact parameter decreases from a large value to a_1, δ/λ_m increases monotonically from 0 to $\frac{1}{3}$. The first term in this series can also be derived by calculating in the impulse approximation the deflection of a particle traveling in a straight line path whose closest distance from the surface is λ_m.

Given β and r_0 we can calculate from Eqs. (7) and (8) the value of λ_m which yields a given deflection s. The values of β used in Table I will be shown to be consistent with our observations of the deflection of a Cs beam by a gold surface of 10-cm radius, and one can see that all the values of λ_m are considerably less than the Cs transition wavelength (≈ 8660 Å).

The intensity per unit width, I, in the detector plane relative to the undeflected beam intensity per unit

TABLE I. Minimum distances of approach of atom to surface ($r_0=10$ cm).

β (10^{-23} cm^3)	Minimum distance to surface (in Å) at deflection s in the detecting plane $s=0.02$ cm	$s=0.06$ cm
5	700	515
7	780	620
12	900	690

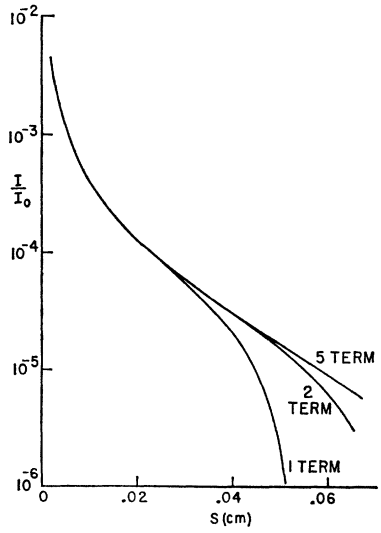

FIG. 2. Theoretical beam profiles for $\beta=6\times10^{-23}$ cm^3 and $r_0=10$ cm. The effect of the number of terms taken in Eqs. (8) and (9) is shown.

[10] D. Raskin, Ph.D. thesis, Columbia University, New York, 1968 (unpublished).

width, I_0, is given by

$$\frac{I}{I_0}=\frac{2}{2-(ds/da)}\approx\frac{2}{-(ds/da)}$$

since the intensities are very small ($I/I_0<\approx 10^{-3}$) for any appreciable deflection ($s>\approx 0.005$ cm). Note that ds/da is intrinsically negative. One then has

$$\frac{I}{I_0}=\frac{4(\lambda_m-3\delta)}{7s+8(s_2+2s_3+3s_4+\cdots)}, \tag{9}$$

where s_n is the nth term in the expression for s [Eq. (8)].

The intensity drops to zero at an s corresponding to $a=a_1$, i.e., when $\delta=\frac{1}{3}\lambda_m$. However, the value of s at which this is calculated to occur depends on the length of the series in Eq. (8). Figure 2 shows the effect of the number of terms taken in the series expansions for s and I/I_0. The values of β and r_0 correspond to a relatively weak force and a large radius. We have typically measured intensities at deflections in the range $0.02\leq s\leq 0.06$ cm because at larger deflections the intensity is too small to measure relative to the noise and background and at small deflections the intensity decreases so rapidly that a small uncertainty in detector position would yield a large error in measured intensity. In the region of useful deflections and for the experimental parameters applicable to our system, the series for s and I/I_0 can be truncated after two terms with no significant loss of accuracy. The effect of r_0 and β on the predicted beam profile in the two-term approximation is shown in Figs. 3 and 4.

The beam of particles of mass M effuses from an oven at a temperature T. The fraction of undeflected particles

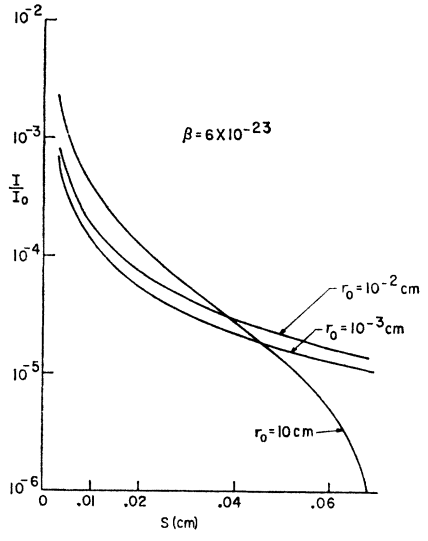

FIG. 3. Theoretical beam profiles for $\beta=6\times10^{-23}$ cm^3 and $r_0=10$, 10^{-2}, and 10^{-3} cm (two-term approximation).

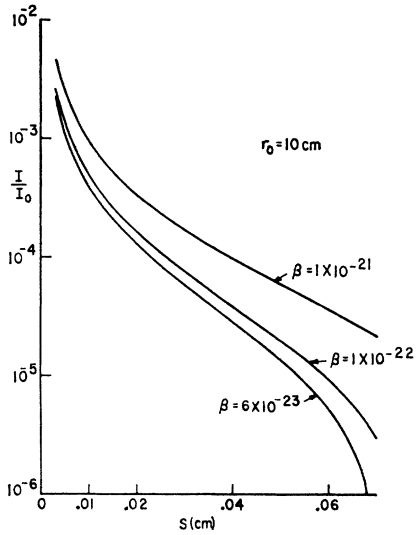

FIG. 4. Theoretical beam profiles for $r_0=10$ cm and $\beta=6\times10^{-23}$, 1×10^{-22}, and 1×10^{-21} cm^3 (two-term approximation).

detected with a velocity between v and $v+dv$ is

$$f(v)dv=2(v/\alpha)^3e^{-(v/\alpha)^2}d(v/\alpha),$$

where

$$\alpha=(2\kappa T/M)^{1/2}\ (\kappa=\text{Boltzmann's constant}).$$

The quantity β is velocity dependent so that the observed beam profile is

$$I(s)=\int_{v=0}^{\infty} I[\beta(v),s]f(v)dv.$$

The integral has been approximately evaluated by considering only the first term in Eqs. (8) and (9). To this approximation $I(s)$ is very nearly $I[\beta(\bar{v}),s]$, where $\bar{v}=1.2\alpha$ and $E_{\text{effect}}=1.4\kappa T$. Since T can be measured directly, the interaction constant k can be found at once from an observed β, since

$$k=\beta E=1.4\kappa T\beta. \tag{10}$$

APPARATUS

The experimental apparatus (Fig. 5) is housed in two stainless-steel chambers whose flanges are sealed with butyl rubber "O" rings. The chambers are separately evacuated by oil-diffusion pumps with water-cooled baffles and liquid-nitrogen vapor traps. The oven and beam shutter are in the source chamber which is connected to the main chamber, in which all other components are located, by a single narrow slit. The ultimate pressure in the main chamber ($\approx 4\times10^{-9}$ Torr as read with a Varian ionization gauge) is not limited by the pressure in the source chamber ($\approx 2\times10^{-7}$ Torr with oven hot). A conventional all-glass gas-handling system is connected to the main chamber through a

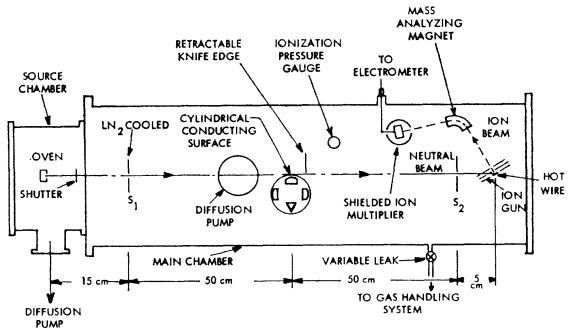

FIG. 5. Experimental system (top view).

variable leak valve for use in studying the scattering of the beam. This system permits research grade gases (N_2, H_2, He, or Ar) to be admitted into the main chamber such that the chamber pressure can be raised stably and reproducibly in increments of less than 5×10^{-10} Torr.

The iron source oven, of conventional design,[11] has an exit slit 0.01 cm wide$\times$0.33 cm high. The temperature of the evaporation is measured by a Chromel-Alumel thermocouple placed in a well in the oven block. The molecular beam of CsCl is produced by heating the oven to 550°C. This temperature corresponds to a vapor pressure[12] of 10^{-2} Torr in the oven. Atomic Cs is produced by the reaction of CsCl with Ca. We have found that an oven temperature of about 400°C will yield a Cs beam whose intensity is approximately that of CsCl evaporated at 550°C.

All the components in the main chamber are mounted on a rigid stainless-steel bench which can be removed from the vacuum envelope so that S_1, S_2, and the deflecting surfaces can be adjusted to parallelism easily and accurately. In addition, the mounting of the critically aligned components on the rigid bench effectively isolates them from any distortions of the vacuum chamber.

The slits S_1 and S_2 used for defining and detecting the beam, respectively, are all-stainless-steel spectroscopic slits (Jarrell-Ash), 10 μ (0.001 cm) wide and $\approx$1.5 cm high. Since S_1 is close to the source, there is a considerable deposition of beam particles on it. It is possible that these particles might creep over the surfaces of the slit jaws to the side facing the detector. If these particles were then reemitted, a significant number of particles would appear in the nominal shadow of the surface. In order to reduce this reevaporation, the slit can be cooled by radiation to a surrounding shield at 77°K. The shield does not make physical contact with S_1 or with any other bench parts.

[11] P. Kusch and V. W. Hughes, in *Handbuch der Physik*, edited by S. Flügge (Springer-Verlag, Berlin, 1959), Vol. 37/1, p. 6.

[12] Landolt-Börnstein, in *Zahlenwerte und Funktionen aus Physik, Chemie, Astronomie, Geophysik und Technik*, edited by A. Eucken (Springer-Verlag, Berlin, 1960), 6th ed., Vol. 2/2a.

The slits S_1 and S_2 are separated by a distance of 100 cm; the deflecting cylinder is located at the midpoint between the two slits. Each of the slits can be moved laterally on three-point roller suspensions on the bench.

Four cylindrical surfaces have been used in the experiment. They are mounted on a rotating table so that any one of the surfaces can be made to protrude into the beam. Two of the surfaces are opaque gold layers ($\approx$2000 Å thick) deposited on 10-cm radius cylindrical glass surfaces each polished to $\frac{1}{4}$ wave on one face of a cube approximately 2 cm on a side (Perkin-Elmer Corp.). Another surface is an uncoated 10-cm radius substrate. The fourth surface is an approximation to a very small radius metal cylinder. It is formed by the edge of a stainless-steel wedge with a vertex angle of 30°. The radius is considered to be an unknown to be determined by experiment. Each of the metal surfaces is electrically grounded.

The table and surfaces are surrounded by a stainless-steel shield which may be heated by attached coils. The assembly of deflecting surfaces may thus be heated uniformly to a temperature of about 300°C. This temperature allows a certain degree of cleaning of the surfaces. Slots are cut in the shield to allow passage of the beam so that experimental data can be taken with the surfaces hot.

The detection unit (Fig. 6) is designed to detect a flux of neutral particles through the detector slit from about 5×10^6 particles per sec in the undeflected beam to as few as 50 pps at large deflection angles. The beam particles that pass through S_2 are ionized at the surface of a hot tungsten ribbon with nearly 100% efficiency. In order to separate the Cs^+ ions from the everpresent background of impurity ions (e.g., Na^+, K^+) evolved from the tungsten filament, the ions are passed through a conventional magnetic mass spectrometer. The field in the $\frac{1}{4}$-in. gap of the magnet is approximately 7500 G.

The ion beam that emerges from the mass-spectrometer exit slit strikes the cathode of a Bendix M-306 ion multiplier. The multiplier is of the resistance strip type and is operated at a measured gain of 6×10^4 for 600-V Cs^+ ions (higher gain is possible).

An input neutral beam flux of 50 pps is converted into an ion beam current of $\approx8\times10^{-18}$ A at the filament.

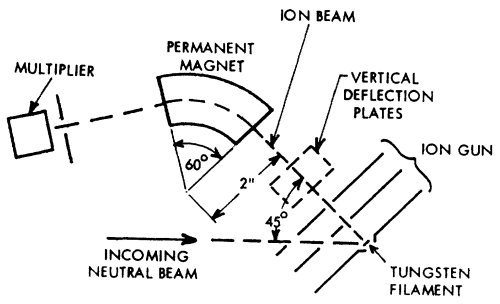

FIG. 6. Detection unit (top view).

About half of this current is lost in the mass spectrometer (mainly because the magnet gap is only half as high as the beam) before the ions reach the multiplier. With the gain of the multiplier, the current becomes $\approx 2.5\times10^{-13}$ A. This current is readily measured with a Keithley 600-A multirange electrometer. The central beam flux corresponds to a current of approximately 2.5×10^{-8} A at the electrometer input; this is also in the range of the electrometer.

The typical background current is $\approx 1\times10^{-14}$ A at the input to the electrometer when the beam shutter is closed but all elements of the detecting unit are on.

METHOD

In the absence of any obstructions in the beam, i.e., if the beam is rotated about the oven slit so that it is not intercepted by the cylinder, the beam profile is approximately trapezoidal with a plateau of uniform intensity I_0, whose width is 0.07 cm in the detector plane. S_1 is then moved laterally towards the deflecting surface until the edge of the surface bisects the region of uniform beam intensity. This is noted through exploration of the profile by motion of S_2 and a corresponding motion of the detector. As S_2 and the ion gun are moved from the plateau into the geometrical shadow of the surface, the intensity drops sharply. The width of the transition from the intensity I_0 to $\frac{1}{2}I_0$ is typically 25 μ (in the detector plane). Of this width, 10 μ result from the finite widths of the slits S_1 and S_2; the remaining 15 μ are presumably due to a very slight lack of parallelism between S_1, S_2, and the edge of the cylindrical surface. Since the transition region is only 0.0025 cm wide and deflections in that region of the profile most sensitive to the interaction potentials are typically 0.02–0.06 cm, the deflection from the edge of the geometrical shadow are known with an accuracy of better than 10%.

The measured beam profile contains a considerable flux of particles that reach the detector through collisions with residual gas molecules in the vacuum chamber. The base pressure of the present experimental system is 4×10^{-9} Torr; calculations based on our data indicate that a pressure of the order of 1×10^{-10} Torr is required if the scattering is to be no more than 10% of the measured signal at deflection angles up to 3.5 min of arc (deflection 0.05 cm). A major problem is to determine the beam profile due to the atom-surface interaction from the measured profile.

Ideally, the intensity at points in the detector plane should be measured as a function of pressure as this is raised in small increments from 4×10^{-9} to about 1.5×10^{-8} Torr. Since the scattered intensity at any angle is proportional to the pressure, one could then extrapolate the observed intensity to zero pressure to find the intensity due to the atom-surface interaction only. This procedure is valid only if the composition of the scattering gas remains unchanged as the pressure is changed. In practice, the admitted gas is not of the same composition as the residual gas, so the method must be modified.

A knife edge parallel to the cylinder axis is brought into the beam on the side opposite to the surface to a position where the width of the beam is drastically reduced but the intensity per unit width immediately adjacent to the knife edge is undiminished (I_0). The effect of the knife edge is to reduce the number of collision sites that have a direct line of sight to the detector. At any deflection angle one may thus find the intensity-versus-pressure line, with the knife edge "in" and with the edge "out." These two lines will include the same atom-surface interaction intensity and will differ only in the scattered intensity. The intensity at the extrapolated point of intersection of the lines is the intensity due only to deflections of the beam by the surface. The actual position "in" is not precisely determined but is very nearly the same in all cases. The only requirement in our extrapolation procedure is that the knife edge remain fixed in the observation of each intensity-versus-pressure line.

Under more rigorous analysis[10] it is found that the validity of the method depends on two assumptions: (1) the pressure gauge is linear without, however, the requirement that the gauge be independent of the gas, and (2) the angular dependence of the differential cross section must in principle be the same for both the residual and admitted gas at small scattering angles without the requirement that the cross sections be the same. Our data indicate that both assumptions are satisfied to a high degree of approximation. The linearity of the ionization gauge is demonstrated by the fact that the plots of intensity versus pressure are linear within experimental uncertainty. The validity of the second assumption is not at all obvious; however, it appears to be satisfied within experimental uncertainty because the interaction intensity I_{inter} as determined by this extrapolation method is independent of the base pressure of the residual gas and of the properties of the admitted gas (H_2, N_2, He, and Ar have been used).

Experimentally we find that the extrapolated intensity I_{inter} is proportional to the central beam intensity I_0. Any contribution to the intensity resulting from self-scattering of the beam would vary quadratically with I_0 (since the beam provides both incident and target particles). Since we do not see a significant variance from linearity, we conclude that, within the experimental uncertainty, self-scattering is negligible.

The deflection of the Cs beam is observed with the defining slit S_1 cooled to near 77°K. With the slit at room temperature, a large extrapolated relative intensity ($I/I_0\approx10^{-4}$) was observed for deflection angles up to and beyond 5 min ($s=0.07$). The measured intensity depends on the position of the ion gun relative to S_2 in the same way as does a beam signal; a signal due to a

general pressure of Cs would be independent of detector position and no such signal has been observed.

It is assumed that this large intensity in the shadow region is due to reevaporation of the Cs beam from the side of S_1 that faces the detector. Considerable amounts of Cs are deposited on the side of S_1 facing the source, and it seems probable that this Cs creeps through the slit and to the back side of the jaws where it evaporates. An atom evaporated from the slit jaw can travel on a straight line to the detector and is thus indistinguishable from a particle that passes through the slit and is deflected into the detector by the surface. The spurious signal can also be expected to fall off rapidly with increasing distance of the point of evaporation from the slit. At 77°K the vapor pressure of Cs is unmeasurably small, and the effect of reevaporation is negligible.

RESULTS

Each of the points in a beam profile is determined by the intersection of two extrapolated lines, each of which is determined from seven data points. The uncertainty in the beam profile resulting from this extrapolation is rather large. Thus, while we have been able to extract the effect of atom-surface interaction from a background of residual gas scattering, we make no claim that our results are definitive. More accurate results await the completion of a new vacuum chamber that will provide a residual pressure low enough to make the extrapolation procedure unnecessary.

Within this limitation of the present apparatus, we report the following observations.

A. Atomic Cs

Data were obtained for a Cs beam interacting with each of the two 10-cm radius gold cylinders and the approximate small radius cylinder made of a stainless-steel wedge. Figures 7 and 8 show two different extrapolations, for which He and Ar were admitted, and which yield the quantity I/I_0 at $s=0.04$ cm for a 10-cm gold surface. The agreement between the two values of I/I_0 is good; the mean value $I/I_0=3.4\times10^{-5}$ has a *statistical* uncertainty of $\pm2.0\times10^{-5}$. It is to be noted that the two values of the "pressure" coordinate ρ_0 of the extrapolated intersection point are widely different. ρ_0 depends on the scattering properties of the injected gas and the residual gas and on the sensitivity of the ionization gauge for the two gases[10] and since it is essentially an algebraic constant and not a real pressure it can be positive and negative. The beam profiles after correction for residual gas scattering are shown in Fig. 9. The profiles for the two 10-cm surfaces are consistent with a theoretical curve corresponding to $\beta=7\times10^{-23}$ cm^3, $r_0=10$ cm. Deviations between the beam profiles for the two surfaces are within the experimental uncertainty. For the stainless-steel wedge, the beam profile is consistent with $\beta=7\times10^{-23}$ cm^3, and $r_0=10^{-3}$ cm, where r_0 is estimated to about a factor of 10. The data are self-consistent since one expects the two values of β to be equal since both surfaces are good conductors.

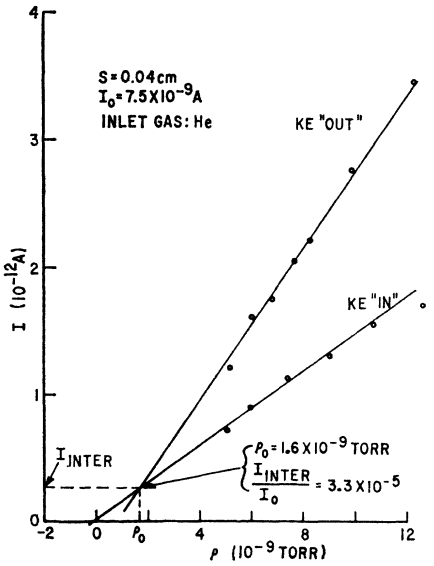

FIG. 7. Typical extrapolation lines for Cs beam and 10-cm gold surface at a deflection $s=0.04$ cm (inlet gas He).

B. CsCl

A beam of CsCl molecules was deflected by each of the three surfaces mentioned in subsection A. Again differences between the profiles for the two gold surfaces are not significant. The data for the large and small radius metal cylinders are consistent with theoretical curves corresponding to $\beta=2\times10^{-22}$ cm^3 with $r_0=10$ cm and $r_0=10^{-3}$ cm, respectively. Note that the

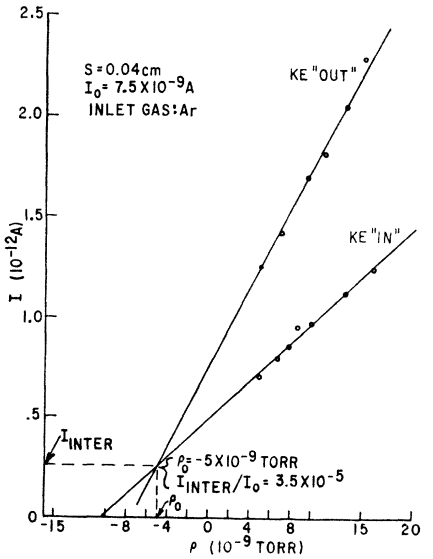

FIG. 8. Typical extrapolation lines for Cs beam and 10-cm gold surface at a deflection $s=0.04$ cm (inlet gas Ar).

data for Cs and CsCl and the cylinder of small and unknown radius may be fitted with the same r_0.

In addition, the CsCl beam was deflected by an uncoated glass cylinder of 10-cm radius. The data for this surface correspond to a curve with $\beta=6\times10^{-23}$ and $r_0=10$. The beam profiles, after correction for scattering, are shown in Fig. 10. The intensity in the shadow region does not depend significantly on the temperature of S_1.

The contribution of scattering to the measured intensity is shown in the results summarized in Table II. In most cases the contribution of the scattered intensity to the total intensity exceeds that due to the dipole interaction. For large deflection angles (large s) the knife edge removes about half of the scattering. Note that the measured intensities at $s=0.02$ and 0.05 cm are approximately the same for both beam materials, but for CsCl more of the intensity is due to the

TABLE II. The measured total relative intensity I_{tot}/I_0, the extrapolated intensity ratio I_{inter}/I_0 due to the atom-surface interaction, and the calculated intensity ratio I_{scat}/I_0 for Cs and CsCl at two positions s, and for the conditions knife edge "in" and "out," $I_{tot}=I_{inter}+I_{scat}$. The base pressure of the system is $\approx5\times10^{-9}$ Torr.

Beam material	Cs		CsCl	
Deflection s (cm)	0.02	0.05	0.02	0.05
$10^5\times I_{tot}/I_0$,				
Knife edge in	25.0	8.0	30.0	7.0
Knife edge out	38.0	15.0	42.0	11.0
$10^5\times I_{inter}/I_0$,	14.0	1.5	21.0	2.9
$10^5\times I_{scat}/I_0$, intensity due to scattering $(=I_{tot}/I_0-I_{inter}/I_0)$, at position s				
Knife edge in	11.0	6.5	9.0	4.1
Knife edge out	24.0	13.0	21.0	8.1
I_{inter}/I_{tot}, at position s				
Knife edge in (%)	56	19	70	41
Knife edge out (%)	37	10	50	26

interaction with the surface. The relation between I_{scat} at $s=0.02$ cm and at $s=0.05$ cm (with knife edge "in" and "out") is consistent with the geometry of the experiment in the approximation that the differential scattering cross section is uniform for all angles less than some value θ_{max} (≈1 mrad) and zero for angles larger than θ_{max}.[13]

The final results are tabulated in Table III. The interaction constant is found from Eq. (10), where T is the oven temperature. Clearly, other theoretical curves pass through the points in Figs. 9 and 10 within the range of experimental uncertainty. In the case of Cs and metal surfaces (Fig. 9), the theoretical curve for $r_0=10$ cm which best fits the tops of the error bars gives $\beta=1.2\times10^{-22}$ (cm^3); that which best fits the lower limits gives $\beta=5\times10^{-23}$. It is reasonable to use these two values as approximate upper and lower bounds for

[13] E. A. Mason, J. T. Vanderslice, and C. J. G. Raw, J. Chem. Phys. 40, 2153 (1964).

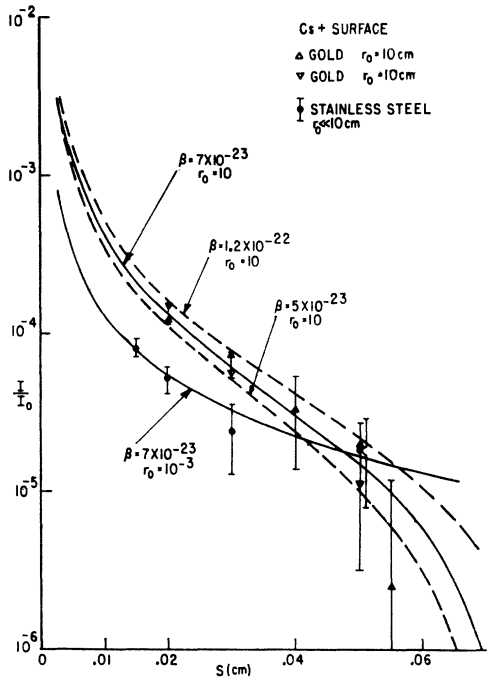

FIG. 9. Experimental beam profiles for Cs. The variance in individual points is that resulting from the extrapolation procedure alone. Theoretical curves in the two-term approximation are drawn in.

β, respectively. The estimated error for the CsCl experiments is also shown in Table III. Note that since the predicted intensity is not a linear function of β, the error is not symmetric.

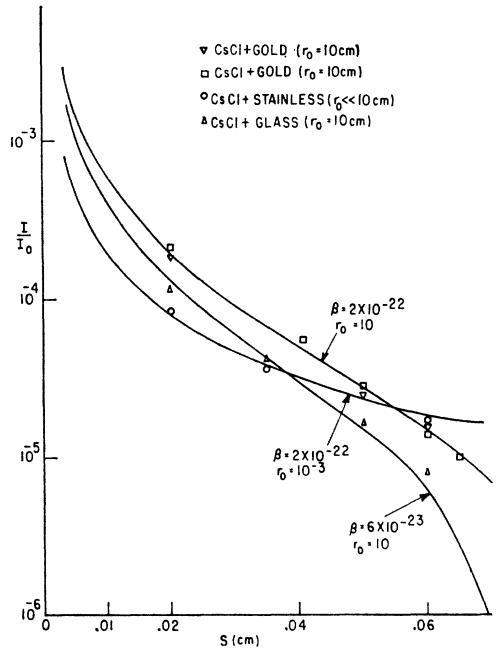

FIG. 10. Experimental beam profiles for CsCl. Theoretical curves in the two-term approximation are drawn in.

TABLE III. Experimental values of the interaction constant k [measured in (Debye)^2].

Beam	Oven temperature T (°K)	Surface	β (cm^3)	k (D^2)
Cs	670	Metal	7×10^{-23}	9_{-3}^{+7}
CsCl	820	Metal	2×10^{-22}	30_{-9}^{+19}
CsCl	820	Glass	6×10^{-23}	10_{-4}^{+8}

The interaction constant for Cs and a metal surface can be examined in terms of the expressions given by Lennard-Jones,[1] Bardeen,[2] and Mavroyannis.[3] In principle all the electrons in the atom ($Z=55$ for Cs) will induce images in the metal, and the interaction between the atom and the surface will be due to all these dipole-dipole interactions (including interactions of one dipole with the image of another). However, since the inner-shell electrons fluctuate at frequencies which are much higher than that of the valence electron, the actual contribution due to the closed shells may be assumed to be considerably less than that of the valence electron. Thus, we will consider only the contribution to the energy of interaction which is due to the valence electron. It is to be noted that in the Lennard-Jones (pure dipole-image) approximation and with an uncorrelated wave function (Slater determinant) for the atom, the interaction between an electron and the image of another electron is repulsive for single-particle states related by $\Delta L=\pm1$ and is zero for all other pairs of states.

The Lennard-Jones interaction constant is given by Eq. (2). We calculate $\langle r^2\rangle_{\rm av}\approx9.5$ Å^2 for the $6s$ valence electron in Cs by using the modified Hartree-Fock-Slater radial wave function calculated by Herman and Skillman.[14] We then find $k_{L-J}=18D^2$. This value is an upper limit on the strength of the interaction if the contribution of inner electrons is ignored.

The value of the interaction constants calculated from the formulas of Bardeen and Mavroyannis [Eqs. (3)–(5)] are $k_{\rm B}=15.5D^2$ and $k_{\rm M}=13.7D^2$, respectively. In evaluating Eqs. (4) and (5) we have used the plasma frequency ($\hbar\omega_p=9$ eV) for gold as given by Pines.[15] We calculate a value of $r_s\approx2$ Å from the plasma frequency; we get the same result using the conduction electron density ($N=2.8\times10^{-22}$ cm^{-3}) given by Shkliarevskii.[16] Both $k_{\rm B}$ and $k_{\rm M}$ agree with the observed value of k within the experimental uncertainty.

In spite of the fact that the interaction between CsCl and a surface is very difficult to evaluate theoretically, it can easily be shown that the permanent dipole-image dipole interaction cannot account for all of the extrapolated deflected intensity.

If μ is the permanent moment [$\mu=10.5D$ for CsCl (Ref. 17)], the interaction constant is

$$k_{\rm perm}=\tfrac{1}{12}\mu^2=9.2\,D^2.$$

This is to be compared with the observed value of $30\,D^2$. The discrepancy is greater than the estimated experimental uncertainty and indicates that the interaction between the surface and the instantaneous electric dipole moments produced by outer electrons of CsCl is of the same order as that for the Cs atom.

We can calculate a rough value for the strength of the interaction between CsCl and a glass surface if we make the following approximations: (a) The motion of the electronic and molecular dipoles is completely uncoupled. That is, $k_D=k_{D\ \rm perm}+k_{D\ \rm inst}$ and $k_C=k_{C\ \rm perm}+k_{C\ \rm inst}$, where the subscripts D and C refer to dielectric and conducting surfaces, respectively. (b) For each contribution (permanent and instantaneous) the relation between k_D and k_C is given by the classical formula

$$k_D=[(\epsilon-1)/(\epsilon+1)]k_C,$$

where ϵ is the dielectric constant of the glass at the appropriate frequency.

We take $k_{C\ \rm perm}=9.2\,D^2$ as calculated above, and thus we have $k_{C\ \rm inst}=20.8\,D^2$, where the latter figure carries the same uncertainty as k_C. We use $\epsilon_{\rm perm}=6$ and $\epsilon_{\rm inst}=2.6$, which are typical dielectric constants for optical glass in the microwave and visible regions, respectively. With these values we calculate

$$k_D=\frac{5}{7}(-9.2)+\frac{1.6}{3.6}20.8=6.5+9.3=15.8D^2.$$

This number is to be compared with the measured value of $10\,D^2$. Clearly, this elementary interpretation of the result is not precluded; no more precise analysis is possible with the present data. The result to be noted is that k_D is significantly less than k_C.

It is possible to exclude the possibility that a number of effects not heretofore considered can contribute significantly to the beam intensity within the geometrical shadow of the surface. (a) There are no stray electric or magnetic fields whose gradients are strong enough to deflect the particles by a meaningful amount. This may be deduced from the known configuration of the elements of the detection system, the only significant source of electric fields, and, in the case of magnetic fields, from the negligible effect of arbitrarily introduced field gradients, much larger than any probable residual gradients in the apparatus. (b) Beam material is, of course, incident on that portion of the cylinder between S_1 and the line on the cylinder which defines the geometrical shadow. No particle that leaves this part of the surface can fall into the geometrical shadow. Those particles that migrate, that are scattered by residual gas, or that are deflected through the process under

[14] F. Herman and S. Skillman, *Atomic Structure Calculations* (Prentice-Hall, Inc., Englewood Cliffs, N. J., 1963).
[15] D. Pines, in *Solid State Physics*, edited by F. Seitz and D. Turnbull (Academic Press Inc., New York, 1955), Vol. 1, p. 435.
[16] I. N. Shkliarevskii and V. G. Padalka, Opt. i Spektroskopiya **6**, 776 (1959) [English transl.: Opt. Spectry. (USSR) **6**, 505 (1959)].
[17] R. G. Luce and J. W. Trischka, J. Chem. Phys. **21**, 105 (1953).

study onto that part of the surface beyond the line that defines the shadow, reevaporate, if at all, into a solid angle so large that no measurable intensity will appear within the shadow. (c) It is possible that a dielectric film (e.g., pump oil) may appear on the conducting surface; but within the range of validity of classical image theory, it can be shown that the beam profile will not be appreciably affected by the film unless its thickness is of the order of the impact parameter of the particle (500 to 1000 Å). Heating the surface to about 250°C would remove all but one or two monolayers ($\approx$10 Å) of a thick film. Since we do not observe a significant change in the beam profile after (or during) heating, we conclude that any dielectric coating of the surface must be a thin one. (d) It is possible that a static electric charge could build up on a nonconductive layer on the surface. The electric field resulting from this charge will be dipolar since an image charge will be induced in the metal surface beneath the insulating area. Since the beam will be deflected only by strong gradients of field, the region of charge would have to be very highly localized. When the effect of this static field is evaluated[10] in the configuration giving rise to the strongest interaction—a very narrow dipole strip parallel to the cylinder axis—and with the dielectric charged to its breakdown strength ($\approx$100 kV/cm), it can be shown that the deflections are much smaller than those resulting from the force under investigation. (e) To test for the presence of ions in the beam, a modest ($\approx$100 V/cm) electric field was applied perpendicular to the beam direction in the region between the interchamber slit and S_1. Since no difference was noted in the measured beam profile when the field was on or off, we conclude that the beam contained only neutral particles. (f) We have not investigated irregularities on the glass cylinders as supplied or on the gold coated cylinders, nor is there any precise description, by the fabricator of the cylinders, of the kinds of irregularities that might be expected to occur on a cylinder polished to within $\frac{1}{4}$ wave ($\approx$1300 Å). This distance is considerably larger than the typical impact parameter, and it is possible that there is a considerable deviation of the effective radius of the cylinder from the nominal radius in the region of closest approach. The data do not suggest that any of these effects are significant within the present capacity for measurement of the beam profile. First, the measured profiles can be described by a value of the cylinder radius r_0, which is consistent with the macroscopic radius of the surface under study. Two nominally identical surfaces do, in fact, yield the same beam profile. Different regions of the cylindrical surface can be investigated by observing beam profiles for various positions of the defining slit S_1, and we have found no significant dependence of the profile on the position of S_1. As was noted earlier (see Fig. 3), the beam profile does not greatly depend on moderate changes in the cylinder radius.

CONCLUSION

There can be no doubt that the deflections measured in this experiment result from an interaction between the surface and the neutral beam. The data are self-consistent and they agree with theoretical predictions based on the modified electric dipole-image dipole potentials proposed by Bardeen and by Mavroyannis. We have been unable to find any extraneous effect other than that of scattering, for which corrections are made, that would cause deflections of the beam that are of the same magnitude as those that we observe.

A more detailed study of the effect described in this paper requires a vacuum system in which an ultimate vacuum better than 10^{-10} Torr can be achieved. If metal surfaces are deposited, *in situ*, by evaporation, the cleanliness of the surface could be much better controlled than in the present experiment.

We are interested in measuring with greater precision the beam profiles for the beam-surface systems discussed in this report. In addition, we intend to investigate the interaction with metal surfaces other than gold to see the effect of resistivity and of the wavelengths at which the absorption bands occur. We are also interested in the effect of the electronic configuration of the ground state of the beam atoms. In particular, we will investigate nonspherical atoms (e.g., thallium—ground state $6s^2 6p\ ^2P$) and atoms with paired electrons in the outer shell (e.g., barium—ground state $6s^2\ ^1S_0$).